

# Studying $\sigma^{54}$ -dependent transcription at the single-molecule level using alternating-laser excitation (ALEX) spectroscopy

M. Heilemann<sup>\*a</sup>, K. Lymeropoulos<sup>a</sup>, S. R. Wigneshweraraj<sup>b</sup>, M. Buck<sup>c</sup>, A. N. Kapanidis<sup>\*a</sup>

<sup>a</sup>Clarendon Laboratory, Department of Physics and IRC in Bionanotechnology, University of Oxford, Oxford, OX1 3PU, United Kingdom

<sup>b</sup>Division of Investigative Sciences, Department of Molecular Microbiology and Infection, Flowers Building, Imperial College London, London SW7 2AZ, United Kingdom

<sup>c</sup>Division of Biology, Sir Alexander Fleming Building, Imperial College London, London, SW7 2AZ, United Kingdom

\*corresponding authors: [m.heilemann1@physics.ox.ac.uk](mailto:m.heilemann1@physics.ox.ac.uk); [a.kapanidis1@physics.ox.ac.uk](mailto:a.kapanidis1@physics.ox.ac.uk); phone 0044 1865-272401; fax 0044 1865-272400

## ABSTRACT

We present single-molecule fluorescence studies of  $\sigma^{54}$ -dependent gene-transcription complexes using single-molecule fluorescence resonance energy transfer (smFRET) and alternating-laser excitation (ALEX) spectroscopy. The ability to study one biomolecule at the time allowed us to resolve and analyze sample heterogeneities and extract structural information on subpopulations and transient intermediates of transcription; such information is hidden in bulk experiments.

Using site-specifically labeled  $\sigma^{54}$  derivatives and site-specifically labeled promoter-DNA fragments, we demonstrate that we can observe single diffusing  $\sigma^{54}$ -DNA and transcription-initiation RNA polymerase- $\sigma^{54}$ -DNA complexes, and that we can measure distances within such complexes; the identity of the complexes has been confirmed using electrophoretic-mobility-shift assays. Our studies pave the way for understanding the mechanism of abortive initiation and promoter escape in  $\sigma^{54}$ -dependent transcription.

**Keywords:** single-molecule fluorescence spectroscopy, single-molecule fluorescence resonance energy transfer (smFRET), alternating-laser excitation (ALEX), sigma54-dependent transcription

## 1. INTRODUCTION

Understanding biomolecular structure and dynamics is central to understanding biological processes. One such process is gene transcription, which uses the multi-functional protein RNA polymerase (RNAP) to copy genetic information from DNA to RNA. In bacteria, RNAP directs transcription after forming a functional complex (“holoenzyme”) with transcription-initiation proteins known as sigma factors; the most common sigma factor is  $\sigma^{70}$  (the “house-keeping” sigma factor) and therefore most of the published work has focused on  $\sigma^{70}$ -dependent transcription [1, 2]; here, we study  $\sigma^{54}$ -dependent transcription, a mode of transcription which operates distinctly from its  $\sigma^{70}$  counterpart [3, 4] [5]. Our goal is to understand how RNAP is regulated by  $\sigma^{54}$  to function in a different way to  $\sigma^{70}$ . Studying  $\sigma^{54}$ -dependent transcription may also explain elements of eukaryotic transcription, since both mechanisms require ATP hydrolysis, specific DNA sequences known as enhancers, and specific activator proteins. Our experimental approach is to study structure and dynamics of

the transcription complexes along the pathway using ensemble and single-molecule fluorescence resonance energy transfer (FRET) spectroscopy of site-specifically labeled proteins and promoter-DNA fragments.

Single-molecule fluorescence spectroscopy is a new family of fluorescence spectroscopy methods that provide information otherwise hidden in the ensemble average [6]. In particular, biomolecular interactions involving many molecules and including several transient states profit from the unique ability of single-molecule fluorescence to uncover subpopulations, observing one complex at a time. A popular single-molecule fluorescence method is single-molecule FRET (smFRET) combined with alternating-laser excitation (ALEX) spectroscopy [7, 8]; this powerful combination recovers information on both distances (via FRET) and interaction stoichiometries in biomolecules. ALEX spectroscopy is well suited to study complex biomolecular interactions both in solution [1, 9] and on surfaces [2], as well as with nanosecond time resolution [10].

Here, we present single-molecule fluorescence studies on regulated transcription-initiation complexes of  $\sigma^{54}$ -dependent transcription. We demonstrate stable complex formation of  $\sigma^{54}$  with promoter DNA fragments, as well as the formation of a “closed” RNAP- $\sigma^{54}$ -DNA transcription complex (a transcription complex in which RNAP- $\sigma^{54}$  interacts intimately with DNA but in which there is incomplete opening of the DNA helix to allow initiation of the transcription reaction). The initial work presented in this manuscript paves the way for further study of  $\sigma^{54}$ -dependent transcription at the single-molecule level, with the ability to identify single steps along the transcription cycle. Apart from its importance for transcription, our work will lead to the development of new general tools for structural biology of large, transient and flexible complexes.

## 2. MATERIALS AND METHODS

### 2.1 $\sigma^{54}$ Protein Expression and Purification

Wild-type  $\sigma^{54}$  and single-cysteine variants C20 and C474 (with a cysteine substitution at position 20 or 474, respectively) were purified as N-terminal His<sub>6</sub>-tagged proteins (pSRW-WT, pSRW-Cys20, pSRW-Cys474; [5]).  $\sigma^{54}$  was overexpressed in BL21-DE3 *Escherichia coli* cells in LB medium in the presence of 50  $\mu$ g/ml kanamycin (Sigma). Cells were grown to OD~0.6 and induced by addition of 0.1 M of isopropyl-1-thio- $\beta$ -D-galactopyranoside (IPTG, Fisher Scientific) and incubation at 37°C for 2h. Cells were harvested by centrifuging them at 10000 g for 30 min at 4°C and the cell pellet was stored at -80°C. Cell pellets were resuspended in ice-cold lysis buffer [Ni-buffer A; 25 mM NaH<sub>2</sub>PO<sub>4</sub> pH 7.0, 500 mM NaCl, and 5% (v/v) glycerol] in the presence of protease inhibitors (Complete, Roche Diagnostics, Basel, Switzerland). Resuspended cells were lysed by sonication, and insoluble material was removed by centrifugation at 18000 g for 30 min at 4°C. For affinity purification, the supernatant was loaded onto a Ni<sup>2+</sup>-precharged, preequilibrated 2-ml HisTrap column (Amersham Biosciences, Piscataway, NJ, USA; see manufacturer’s instructions for column preparation). Nonspecifically bound proteins were removed by washing the column with 0.05 M imidazole in Ni-buffer A. The His<sub>6</sub>-tagged  $\sigma^{54}$  was eluted with 0.6 M imidazole in Ni-buffer A and dialyzed overnight against storage buffer [10 mM Tris-HCl pH 8.0, 50 mM NaCl, 0.1 mM EDTA, 1 mM DTT, and 50% (v/v) glycerol] at 4°C. Aliquots were stored at -80°C.

### 2.2 Fluorescent Labeling of Single-Cysteine Derivatives of $\sigma^{54}$

Purified single-cysteine derivatives of  $\sigma^{54}$  (C20 and C474) were labeled with Cy3B using 10-fold excess of Cy3B-maleimide (Amersham Biosciences) in 0.1 M sodium phosphate pH 7.5, 1 mM EDTA, for 4 h at room temperature. The reaction mixture was loaded onto a ToyoPearl-50F gel filtration column (Sigma) equilibrated with storage buffer [20 mM Tris-HCl pH 7.9, 100 mM KCl, 0.1 mM EDTA, 0.1 mM DTT]. Peak fractions of eluted  $\sigma^{54}$  were collected, and glycerol was added to a final concentration of 50% for storage at -

20°C. Concentrations were determined using UV-Visible spectroscopy (for all  $\sigma^{54}$  derivatives,  $\epsilon_{280\text{nm}} \sim 42500 \text{ l mol}^{-1} \text{ cm}^{-1}$ ). Labeling efficiencies of 80 to 95% were obtained.

### 2.3 Promoter DNA Fragments

Synthetic DNA oligonucleotides corresponding to -35 to +20 of the *Sinorhizobium meliloti nifH* promoter sequence were ordered from IBA (Goettingen, Germany). Mismatches at positions -12/-11 or between positions -10 and -1 in the top strand were introduced, in order to mimic early- or late-melted promoter conformations. The bottom strand DNA was modified with a C6-amino linker either at the 3'- or 5-end, allowing for fluorophore labeling. The bottom strand was labeled with ATTO647N (ATTO-TEC GmbH, Siegen, Germany) according to the manufacturer's protocol and purified on a reversed phase C18 column ( $\mu$ RPC C2/C18, Amersham Biosciences) on a liquid chromatography system (AKTA, Amersham Biosciences).

### 2.4 Native Gel Mobility Shift Assays

Reactions were conducted in STA buffer [25 mM Tris-acetate, pH 8.0, 8 mM Mg-acetate, 10 mM KCl, 1 mM DTT, and 3.5% (w/v) poly-ethylene glycol (PEG-6000)] in a final volume of 10  $\mu$ l at 37°C with 200 nM DNA, 300 nM RNAP core (Epicentre, Madison, WI, USA) and 350 nM  $\sigma^{54}$ . For electrophoresis, reactions were loaded onto a 5% (w/v) native polyacrylamide Bio-Rad Mini-Protean gel (BioRad, Hercules, CA, USA). Gels were run in TG buffer [25 mM Tris, 200 mM Glycine, pH 8.6] for 60 min at 80 V at room temperature. Gels were imaged with a laser gel scanner (PharosFX, BioRad; laser wavelengths 532 nm and 635 nm), and bands were assigned to various complexes according to their mobility and fluorescence properties.

### 2.5 FRET Assays and Distance Calculation

Ensemble fluorescence measurements were conducted using a PTI fluorescence spectrophotometer (PTI, Birmingham, NJ, USA) using excitation wavelengths of 530 nm for Cy3B and 620 nm for ATTO647N. Assays were performed in a microcuvette of 50  $\mu$ l volume and 10 mm path length, using identical concentrations as described for native gel mobility shift assays (section 2.4).

The values of FRET efficiency  $E$  were calculated using the sensitized-acceptor method ([11]; the method takes into account the direct excitation of the acceptor and the crosstalk of the donor fluorophore). Spectra were further corrected for detection efficiency of the spectrophotometer. The separation between donor and acceptor was calculated from FRET efficiencies using  $R = R_0((1/E)-1)^{1/6}$ , with  $R_0 = 6.5 \text{ nm}$  for the dye pair of Cy3B and ATTO647N derived from spectral data [11].

### 2.6 Single-Molecule Fluorescence Spectroscopy: Data Acquisition and Analysis

Single-molecule fluorescence experiments were carried out using smFRET and two-color ALEX spectroscopy in solution with excitation wavelengths of 532 nm and 635 nm, following published experimental protocols [8, 12]. Briefly, two alternating continuous-wave laser sources (532 nm, Samba, Cobolt, Sweden; 635 nm, Cube, Coherent, USA) were coupled into an inverted confocal microscope (IX71, Olympus, Japan). Data acquisition was performed with custom written software (LabVIEW 7.1; National Instruments, Austin, TX, USA); a modulation frequency of 10 kHz was applied. Fluorescence arrival times were recorded on two spectrally-separated detectors (SPQR-14, Perkin Elmer, Fremont, CA, USA) and processed using custom LabVIEW software. A schematic of the setup is shown in Figure 1a.

Stoichiometries  $S$  and uncorrected FRET efficiencies  $E^*$  were calculated for each fluorescence burst above a certain threshold, according to published protocols [1, 8], yielding two-dimensional  $E^*$ - $S$  histograms that allow identification and sorting of subpopulations (see Fig.1b).

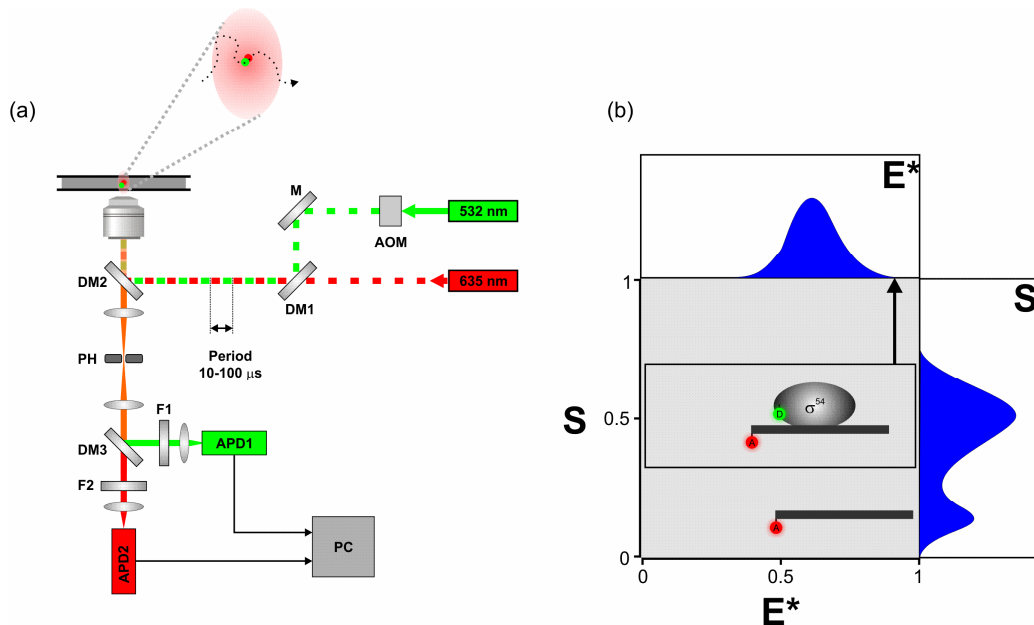


Fig. 1. (a) Experimental setup. Abbreviations: AOM, acousto-optical modulator; M, mirror; DM, dichroic mirror; PH, pinhole; F, filter; APD, avalanche photodiode. The sample in the observation volume is illuminated by two rapidly modulated lasers, 532 nm and 635 nm. Fluorescence emission is directed toward photodiode detectors, and processed by a PC. (b) Two-dimensional histogram sorts molecules according to stoichiometry  $S$  and energy transfer  $E^*$  (donor-only species were removed for clarity).

### 3. RESULTS AND DISCUSSION

#### 3.1 Heteroduplex DNA Promoter Fragments

We are interested in interactions of RNAP,  $\sigma^{54}$  and DNA, and we aim to answer structural and mechanistic questions in  $\sigma^{54}$ -dependent transcription, which involved a complex interplay of several proteins with DNA. Here, we investigate the structure of  $\sigma^{54}$  and RNAP- $\sigma^{54}$  bound to *S. meliloti nifH* promoter fragments (Fig. 2a) using FRET, both at the ensemble and single-molecule levels.

To form stable protein-DNA complexes of  $\sigma^{54}$  and promoter DNA, we used heteroduplex promoter fragments labeled either at the 3'- or 5'-end of the bottom strand with fluorophore ATTO647N. Mismatched base pairs generate a bubble in the duplex and thus facilitate binding of  $\sigma^{54}$  to DNA, stabilizing the complexes [13]. The early-melted promoter fragment with a 2-base mismatch at positions -12 and -11 promotes binding of  $\sigma^{54}$  to DNA and the formation of a closed complex. The late-melted promoter fragment with a 10-base mismatch between positions -10 and -1 mimics the transcription bubble (the form of promoter DNA that transiently becomes single-stranded to allow RNAP to initiate transcription by “reading” the DNA sequence in the template DNA strand) and facilitates the formation of an open complex (Fig. 2b).

To study  $\sigma^{54}$ -dependent transcription, we use FRET between a donor-labeled site in  $\sigma^{54}$  and an acceptor-labeled site in a heteroduplex promoter DNA fragment; the FRET donor and acceptor were fluorophores

Cy3B and ATTO647N, respectively. Depending on the geometric arrangement of the fluorophores, we distinguish two possible scenarios: trailing-edge FRET and leading-edge FRET.

In the trailing-edge FRET case (Fig. 2C, left), the FRET donor is placed close to the RNAP “trailing-edge” ( $\sigma^{54}$  labeled at position 474, close to the C-terminus), whereas the FRET acceptor is placed *upstream* of the DNA interacting with the trailing-edge (DNA labeled at position -35).

(a)

*Sinorhizobium meliloti nifH* promoter (-35 to +20)



(b)

Early-melted sequence (mismatch at positions -12/-11) labelled at position -35:



Early-melted sequence (mismatch at positions -12/-11) labelled at position +20:



Late-melted sequence (mismatch at positions -10/-1) labelled at position -35:

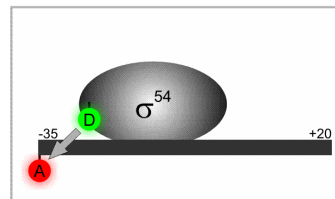


Late-melted sequence (mismatch at positions -10/-1) labelled at position +20:



(c)

Trailing-edge FRET



Leading-edge FRET

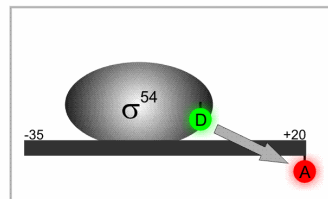


Fig. 2. (a) *S. meliloti nifH* promoter (bases -35 to +20). (b) Heteroduplex promoter fragments, labeled with ATTO647N at the 3'-end or 5'-end of the bottom strand. The numbering refers to the distance (in basepairs) from the transcription start site; negative numbers denote a base in the upstream direction, where positive numbers denote a base in the downstream direction. (c) Principle of trailing-edge and leading-edge FRET.

In the leading-edge FRET (Fig. 2C, right), the FRET donor is placed close to the RNAP “leading-edge” ( $\sigma^{54}$  labeled at position 20, close to the N-terminus), whereas the FRET acceptor is placed *downstream* of the DNA interacting with the leading-edge (DNA labeled at position +20).

DNA-cleavage studies that reveal proximity between sites in  $\sigma^{54}$  and DNA [14] have shown that our chosen trailing-edge  $\sigma^{54}$  site (C474) is in close proximity with bases -32 to -28 on the bottom strand, whereas our chosen leading-edge  $\sigma^{54}$  site (C20) is in close proximity with bases -16 to -11 on the top strand. With the set of heteroduplex promoter DNA fragments used in our experiments, we expect high FRET for the trailing-edge FRET experiment, and low FRET for the leading-edge FRET experiment.

### 3.2 Gel Mobility Shift Assays

We first examined the influence of introducing a fluorophore in each single-cysteine  $\sigma^{54}$ -derivatives and at either end of heteroduplex DNA on the biochemical activity of the biomolecules. We performed electrophoretic-mobility shift assays (EMSA) with wild-type  $\sigma^{54}$ , unlabelled single-cysteine  $\sigma^{54}$  derivatives and single-cysteine  $\sigma^{54}$  derivatives labeled with Cy3B.

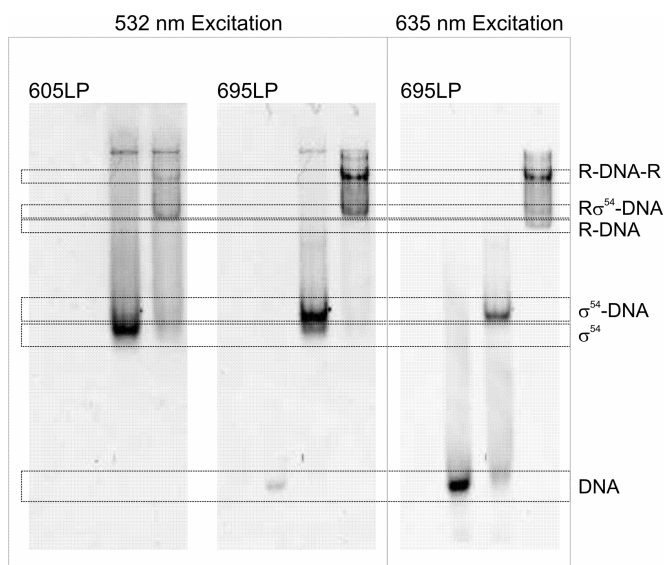


Fig. 3. EMSA of  $\sigma^{54}$  (labeled with Cy3B at cysteine-residue 474) and early-melted DNA. Gel was scanned with two excitation wavelengths (532 nm and 635 nm; sequential scans) to detect the donor-species and acceptor-species (605LP and 695LP), as well as FRET (532 nm excitation and 695LP emission). Bands were assigned according to mobility and fluorescence signal. “R” stands for core RNAP.

Gels were analyzed with a gel scanner, and bands were assigned to different complexes. Exemplary gel scan images with  $\sigma^{54}$  (labeled at position C474 with Cy3B) and early-melted DNA (labeled at position -35 with ATTO647N) are shown in Figure 3.

The fluorescence emission of the bands on different channels, together with the FRET signal, allowed us to assign bands to various species (Fig. 3, right). Complexes  $\sigma^{54}$ -DNA and R- $\sigma^{54}$ -DNA can be easily identified, indicating that complex formation is not perturbed by fluorophore labeling. Most of the free DNA shifts to the  $\sigma^{54}$ -complex in the presence of  $\sigma^{54}$  and DNA only; all DNA is shifted in the presence of  $\sigma^{54}$ -holoenzyme

( $R\sigma^{54}$ ). The EMSA results indicate strong binding both for  $\sigma^{54}$ -DNA as well as  $R\sigma^{54}$ -DNA (in good agreement to published work using similar labeled DNA and sigma54-derivatives [15]).

### 3.3 Ensemble FRET

We used fluorescence-intensity measurements, and in particular trailing-edge and leading-edge FRET (section 3.1; Fig. 2c), to detect formation of protein-DNA complexes and obtain structural information about intramolecular distances.

The ensemble fluorescence spectra for both trailing-edge and leading-edge FRET experiments (section 3.1; Fig. 2c) with the early-melted promoter fragment are shown in Figs. 4a and 4b, respectively. Corrected FRET efficiencies of  $E = 0.46$  and  $E = 0.16$  are obtained using the sensitized-acceptor method (section 2.5).

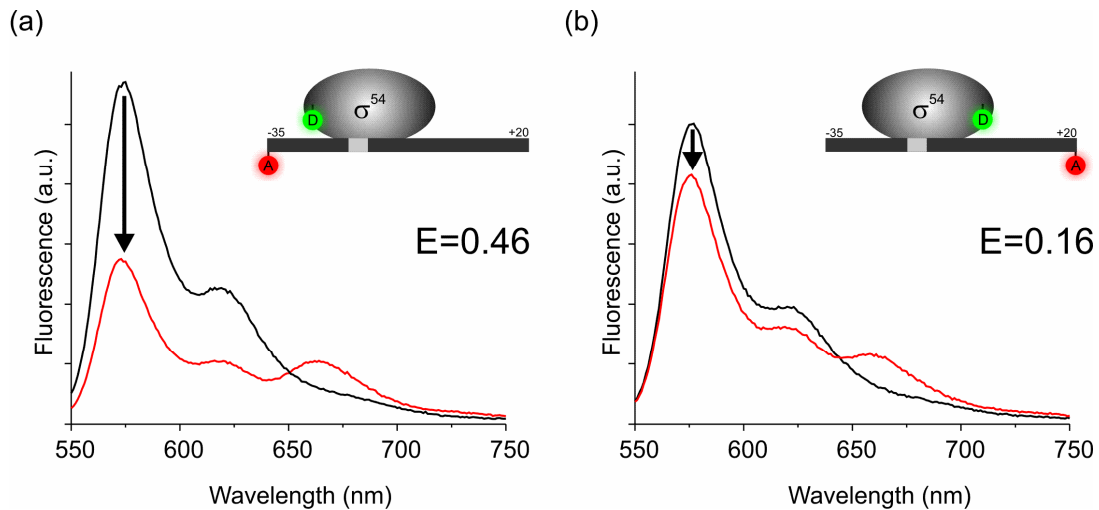


Fig. 4. Addition of acceptor-labeled DNA to donor-labeled protein cause FRET-induced quenching of the donor fluorescence. Emission spectrum of free  $\sigma^{54}$ , black curve; emission spectrum of  $\sigma^{54}$  plus DNA, red curve. (a) Trailing-edge FRET experiment:  $\sigma^{54}$  (C474 labeled with Cy3B) and early-melted DNA labeled at position -35. (b) Leading-edge FRET experiment:  $\sigma^{54}$  (C20 labeled with Cy3B) and early-melted DNA labeled at position +20.

Ensemble fluorescence data inevitably suffer from averaging. For both ensemble-FRET experiments (Fig. 4), the solution also contains free DNA fragments, a fact that can be seen from the gel assays (Fig. 3). As a consequence, the observed ensemble  $E$  is lower than the expected  $E$  for the isolated  $\sigma^{54}$ -DNA complex.

We note that any experiment aiming at studying the formation of a closed complex or active transcription complexes faces an even more heterogeneous mixture of various complexes (Fig. 3). The general problem of ensemble averaging can be circumvented by using single-molecule fluorescence techniques.

### 3.4 $\sigma^{54}$ -DNA Complexes at the Single-Molecule Level

To overcome ensemble averaging, we studied  $\sigma^{54}$ -DNA interactions at single-molecule conditions in solution, observing smFRET and sorting molecules by their stoichiometry using ALEX.

Two-dimensional  $E^*$ - $S$  histograms of leading-edge and trailing-edge FRET experiments at the single-molecule level are shown in Fig. 5a and 5b, respectively. Next to a dominant acceptor-only population in both experiments ( $S \sim 0.2$ ), a low-FRET population for the leading-edge experiment and a high-FRET population for the trailing-edge experiment, both around  $S \sim 0.5$ , can be identified. Approximately 6% of leading-edge FRET complexes and  $\sim 7\%$  of trailing-edge complexes are observed (with respect to free DNA).

A collapse of  $E^*$  for all donor-acceptor species (events within  $S = 0.5-0.9$ ; black boxes in  $E^*$ - $S$  histograms in Fig. 5), yields a single population for each experiment, with mean  $E^* \sim 0.19$  in the leading-edge FRET experiment, and  $E^* \sim 0.88$  in the trailing-edge FRET experiment. Approximate distances of 8.3 nm and 4.7 nm are derived from mean  $E^*$  values, respectively. However, to determine distances from corrected FRET efficiencies, a number of corrections are required such as subtraction of crosstalks due to direct excitation of the acceptor, leakage of the donor, as well as a correction factor for detection efficiencies [12]. We obtained corrected  $E$  values of 0.17 (8.5 nm) and 0.92 (4.3 nm), respectively.

Comparing single-molecule data to ensemble FRET experiments presented in section 3.3 and in Fig. 4, it becomes evident that it will be very challenging to extract structural information from an ensemble experiment.

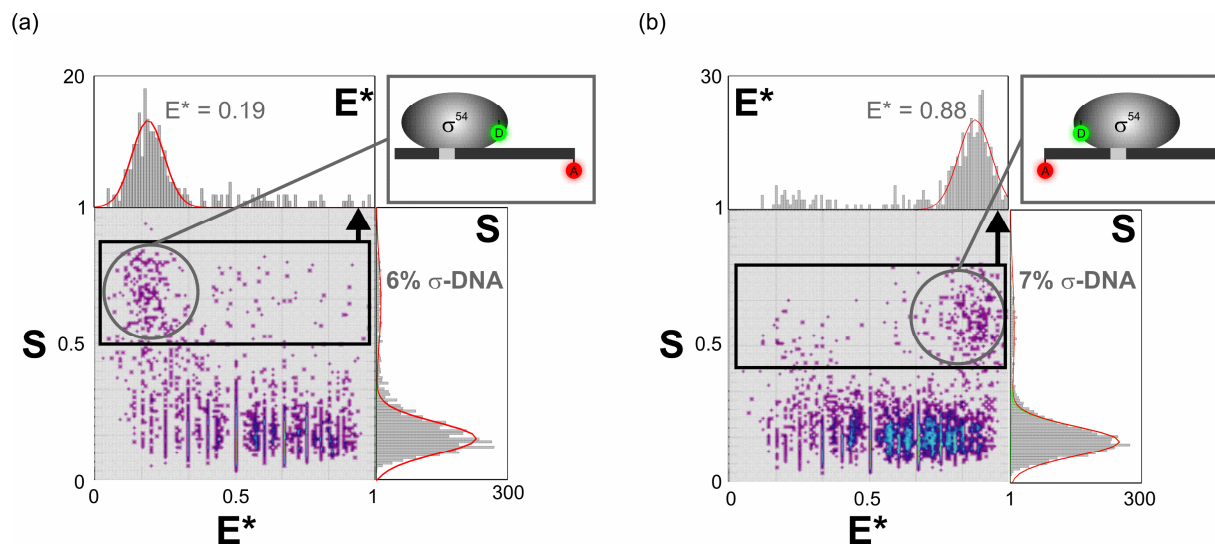


Fig. 5. (a)  $E^*$ - $S$  histogram of a leading-edge FRET experiment:  $\sigma^{54}$  (C20 labeled with Cy3B) and early-melted DNA (labeled at position +20 with ATTO647N). (b)  $E^*$ - $S$  histogram of a trailing-edge FRET experiment:  $\sigma^{54}$  (C474 labeled with Cy3B) and early-melted DNA (labeled at position -35 with ATTO647N).

### 3.5 $R\sigma^{54}$ -DNA Complexes at the Single-Molecule Level

In a further step, we investigated the formation of closed complexes  $R\sigma^{54}$ -DNA, i.e. the interaction of heteroduplex promoter fragment with  $R\sigma^{54}$ -holoenzyme. The collapse of  $E^*$  of closed complexes formed with early-melted and late-melted DNA in trailing-edge experiments (with  $\sigma^{54}$  labeled at C474 with Cy3B) are shown in Fig. 6a and 6b.

Compared to single-molecule data for  $\sigma^{54}$  binding DNA presented in section 3.4 and Fig. 5, the stability of closed complexes at the single-molecule level is significantly higher, i.e. 23% for early-melted DNA and 16%

for late-melted DNA.  $E^*$  values obtained are similar, 0.86 and 0.90, but a broader population is observed for early-melted DNA which might also be interpreted as a second population. The closed complexes are stable over the course of data acquisition (15-20 min).

We conducted similar experiments with homoduplex promoter fragment (data not shown). Consistently with biochemical data, the stability of the complexes is lower and only  $\sim 0.1 - 0.5\%$  of the promoter DNA is involved in formation of the closed complex; importantly, these species exhibited  $E^*$  values similar to the ones obtained using heteroduplex DNA.

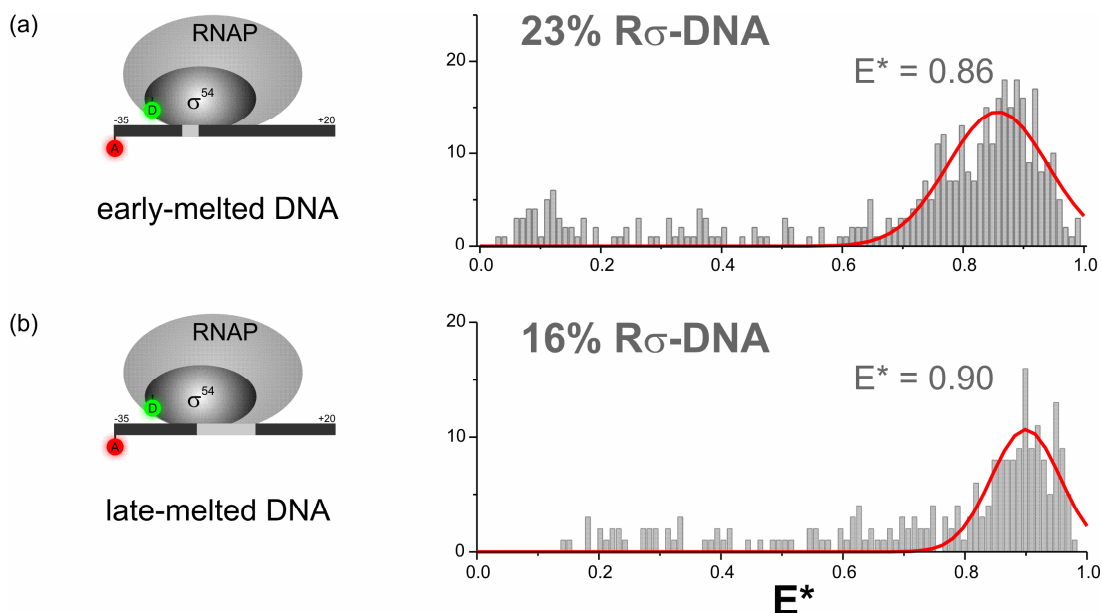


Fig. 6. (a) Trailing-edge FRET experiment: closed complex formed with RNAP- $\sigma^{54}$  (C474 labeled with Cy3B) and early-melted DNA (labeled at position -35 with ATTO647N). (b) Trailing-edge FRET experiment: closed complex formed with RNAP- $\sigma^{54}$  (C474 labeled with Cy3B) and late-melted DNA (labeled at position -35 with ATTO647N).

The fact that the approximate distances obtained using our single-molecule FRET approach are consistent with ensemble FRET [15] and DNA-cleavage studies [14] on similar complexes validates our approach and paves the way for numerous single-molecule studies on the mechanism and kinetics of  $\sigma^{54}$ -dependent transcription.

#### 4. CONCLUSION AND OUTLOOK

We presented a method that allows studying the structure of  $\sigma^{54}$ -dependent transcription complexes. Specifically, we demonstrated a method to derive structural information on various complexes of  $\sigma^{54}$  and  $\sigma^{54}$ -holoenzyme with heteroduplex promoter DNA, without averaging as observed in bulk experiments, by using smFRET and ALEX spectroscopy. The method we present is ideally suited for further studies on  $\sigma^{54}$ -dependent transcription, a complex and heterogeneous interplay of proteins and DNA.

The present single-molecule work can be extended to study complex steps in the transcription pathway (e.g., the formation of transcriptionally-active open complexes and transcription-initiation complexes), and to address the question of  $\sigma^{54}$ -retention in transcription elongation. Our studies will also benefit from use of three-color ALEX spectroscopy, which can increase substantially the structural information obtained from transcription complexes [16].

## ACKNOWLEDGEMENTS

This work was funded by EPSRC grant EP/D058775, Marie Curie EU grant MIRG-CT-2005-031079 and by a UK Bionanotechnology IRC grant. M.H. was supported by a DAAD fellowship.

## REFERENCES

1. Kapanidis, A.N., et al., *Retention of transcription initiation factor sigma70 in transcription elongation: single-molecule analysis*. Mol Cell, 2005. **20**(3): p. 347-56.
2. Margeat, E., et al., *Direct observation of abortive initiation and promoter escape within single immobilized transcription complexes*. Biophys J, 2006. **90**(4): p. 1419-31.
3. Buck, M. and W. Cannon, *Specific binding of the transcription factor sigma-54 to promoter DNA*. Nature, 1992. **358**(6385): p. 422-4.
4. Buck, M., et al., *The bacterial enhancer-dependent sigma(54) (sigma(N)) transcription factor*. J Bacteriol, 2000. **182**(15): p. 4129-36.
5. Burrows, P.C., et al., *Reorganisation of an RNA polymerase-promoter DNA complex for DNA melting*. Embo J, 2004. **23**(21): p. 4253-63.
6. Weiss, S., *Fluorescence spectroscopy of single biomolecules*. Science, 1999. **283**(5408): p. 1676-83.
7. Kapanidis, A.N., et al., *Fluorescence-aided molecule sorting: analysis of structure and interactions by alternating-laser excitation of single molecules*. Proc Natl Acad Sci U S A, 2004. **101**(24): p. 8936-41.
8. Kapanidis, A.N., et al., *Alternating-laser excitation of single molecules*. Acc Chem Res, 2005. **38**(7): p. 523-33.
9. Kapanidis, A.N., et al., *Initial transcription by RNA polymerase proceeds through a DNA-scrunching mechanism*. Science, 2006. **314**(5802): p. 1144-7.
10. Laurence, T.A., et al., *Probing structural heterogeneities and fluctuations of nucleic acids and denatured proteins*. Proc Natl Acad Sci U S A, 2005. **102**(48): p. 17348-53.
11. Clegg, R.M., *Fluorescence resonance energy transfer and nucleic acids*. Methods Enzymol, 1992. **211**: p. 353-88.
12. Lee, N.K., et al., *Accurate FRET measurements within single diffusing biomolecules using alternating-laser excitation*. Biophys J, 2005. **88**(4): p. 2939-53.
13. Cannon, W., S.R. Wigneshweraraj, and M. Buck, *Interactions of regulated and deregulated forms of the sigma54 holoenzyme with heteroduplex promoter DNA*. Nucleic Acids Res, 2002. **30**(4): p. 886-93.
14. Burrows, P.C., et al., *Mapping sigma 54-RNA polymerase interactions at the -24 consensus promoter element*. J Biol Chem, 2003. **278**(32): p. 29728-43.

15. Leach, R.N., et al., *Mapping ATP-dependent activation at a sigma54 promoter*. J Biol Chem, 2006. **281**(44): p. 33717-26.
16. Lee, N.K., et al., *Three-color alternating-laser excitation of single molecules: monitoring multiple interactions and distances*. Biophys J, 2007. **92**(1): p. 303-12.